UDK 625.821.4:539.217
Original scientific article/Izvirni znanstveni članek

ISSN 1580-2949
Mater. Tehnol.

APPLICATION OF GROUND GRANULATED BLAST-FURNACE SLAG IN WASTE ROCK-TAILINGS CEMENTED BACKFILL OF A COPPER MINE

UPORABA MLETE GRANULIRANE PLAVŽNE ŽLINDRE V ODPADNEM ZASIPU Z JALOVINO IZ RUDNIKA BAKRA

Weicheng Ren[1,2,*], Shuo Zhang[1,2], Chao Li[3]

[1]School of Environmental Science and Safety Engineering, Tianjin University of Technology, Tianjin 300384, China
[2]Tianjin Key Laboratory of Hazardous Waste Safety Disposal and Recycling Technology, Tianjin 300384, China
[3]Tianjin Jinneng Binhai Thermal Power Co., LTD., Tianjin Energy Group, Tianjin 300450, China

Prejem rokopisa – received: 2025-02-21; sprejem za objavo – accepted for publication: 2025-09-18

doi:10.17222/mit.2025.1402

This research investigates the feasibility of utilizing ground granulated blast-furnace slag (GGBS), crushed stone and copper tailings (CTs) for cemented paste backfill. Experiments were conducted with waste rock and CTs as aggregates, in a ratio of 6:4, along with various combinations of GGBS and cement as binders. The influence of the GGBS proportion on the consolidation of backfill was also explored. The unconfined compressive strength (UCS), the tensile strength (TS) and the ASTMC1202 of electric flux were all tested and used in the analysis of backfill characteristics. The results show that (i) under standard curing conditions, after 28 days of cement hardening, ground granulated blast-furnace slag (GGBS) continues to hydrate, exhibiting a strength effect that results in a strength increase range of 14–38 %; (ii) the addition of mineral powder to concrete can reduce the hydration heat of the paste; (iii) for the same curing time, the migration charge of the concrete test block decreases with the increase in the GGBS content, while for the same GGBS content, the migration charge of the test block decreases with the increase in the curing time; (iv) as the GGBS's activating effect gradually develops, the interfacial forces and diffusion process at the adjacent boundaries become active, and the hydration reaction rate increases, improving the later strength of the fill material. Based on these results, it was concluded that GGBS can be utilized as a binder when a gravel-tailings aggregate mixture is used as the backfill material.

Keywords: ground granulated blast-furnace slag (GGBS), copper tailings (CTs), impermeability, hydration and heat release, cemented backfill

V članku avtorji opisujejo raziskavo uporabnosti mlete granulirane plavžne žlindre (GGBS; angl.: ground granulated blast-furnace slag), zdrobljenega kamenja in bakrenih odpadkov (CTS; angl.: copper tailings) za cementirani povratni zasip. Nekaj preizkusov so avtorji izvedli z odpadnim kamenjem in CTS v agregatnem razmerju 6:4 v kombinaciji z različnimi deleži GGBS in vezivnega cementa. Nato so ugotavljali vpliv deleža dodane GGBS na konsolidacijo (utrditev) zasipa. Določili so karakteristike zasipa in sicer: končno tlačno trdnost (UCS; angl.: unconfined compressive strength), natezno trdnost (TS; angl.: tensile strength) in električni fluks v skladu s standardom ASTMC1202. Rezultati so pokazali da: (i) pri standardnih pogojih utrjevanja (28 dni cementiranja) GGBS nadalje hidrira, kar povzroči utrjevalni efekt in naraščanje trdnosti za med 14 % in 38 %, (ii) dodatek mineralnega prahu k cementu zmanjša učinek sproščanja toplote zaradi hidracije, (iii) pri enakem načinu staranja se migracija električnih nabojev v betonskem preizkusnem bloku zmanjšuje z naraščanjem dodatka GGBS, medtem ko se pri enaki vsebnosti GGBS migracija nabojev v preizkusnem bloku zmanjšuje s povečevanjem časa staranja, (iv) ko postopoma začne delovati aktivacijski učinek pepela, se aktivirajo sila in difuzijski procesi med mejami kristalnih zrn oziroma agregatov. Tako hitrost hidracijske reakcije narašča, kar izboljša kasnejšo trdnost zasipa. Na osnovi rezultatov te raziskave avtorji v zaključkih ugotavljajo, da se GGBS lahko uporablja kot vezivo, kadar se mešanica agregatov iz gramoza in jalovine uporablja kot material za zasipanje.

Ključne besede: mleta granulirana plavžna žlindra, odpadki iz rudnika bakra, neprepustnost, hidracija in sproščanje toplote, cementirano zasipanje

1 INTRODUCTION

Granulated blast-furnace slag (GBS) is the waste residue produced in smelting pig iron.[1] The annual output of GBS is large, but its comprehensive utilization rate is insufficient.[2,3] Relevant studies have found that slag has a gelation activity similar to that of cement.[4,5] Silicate and silicaluminate as the main components of molten iron floating on the surface are generated in the process of blast-furnace ironmaking.[6–8] The molten slag is regularly discharged from the slag outlet and then granulated by cold air or water treatment.[9,10] GGBS is a powder which is dried and pulverized to reach a certain fineness, conforming to the corresponding activity index.[11] GGBS exhibits potential hydraulic strength and high concrete activity, and is a high-quality admixture for cement and concrete.[12,13]

GGBS has been widely used along with the development of grinding technology and the rise of premixed concrete.[14,15] The use of GGBS to partially or completely replace cement-bonded fine tailings from mines in preparing filling bodies, on the one hand, helps to improve

*Corresponding author's e-mail:
renweicheng@email.tjut.edu.cn (Weicheng Ren)

the filling strength,[16,17] and on the other hand, it can save the amount of cement used, thus greatly reducing the filling cost.[18,19] There have been many studies on the effect of GGBS replacing part of the cement on concrete performance. Reddy Suda and Srinivasa Rao maintain that certain combinations of microsilica (MS) and GGBS can enhance the strength of concrete when compared to MS and GGBS alone.[20] Min Chendi, and Shi Ying, among others, conducted research on the performance of phosphogypsum cemented filling bodies using composite Portland cement (PC) and ground granulated blast-furnace slag (GGBFS) as binders. They found that phosphogypsum interferes with the hydration of the binder, and that using PC-GGBFS as a binder results in higher strength compared to using pure PC.[21] Li Kai and Zhu Lishun, among others, used phosphogypsum (PG) as a raw material, combined with steel slag (SS) and ground granulated blast-furnace slag (GGBS), under the action of an alkali activator (NaOH) to prepare a fully solid waste phosphogypsum-based backfill material (PBM). They studied the effects of the slag-to-slag ratio on the compressive strength and toxicity leaching of PBM.[22] T. Mashifana et al. found that the particle size distribution influences the strength development of granulated blast-furnace slag-modified gold tailings.[23] N. Ouffa et al. investigated the potential of ground granulated ladle furnace slag (GGLFS) as a partial replacement for general-use Portland cement (GU) and ground granulated blast-furnace slag (GGBFS) in cemented paste backfill (CPB). GGLFS accelerates the initial reaction and alters the hydration products in GU/GGBFS formulations.[24] However, there are still relatively few researches on the influence of the inclusion of GGBS on the durability and impermeability of backfill. The impermeability and composition of hydration reaction products in backfill materials significantly influence their mid-to-late stage strength. Therefore, investigating the effects of the GGBS content on the impermeability and hydration reactions of backfill materials holds critical research significance.

2 EXPERIMENTAL PART

2.1. Materials

The experimental materials are ground granulated blast-furnace slag (GGBS), crushed stone, graded tailings and Portland cement.

(1) GGBS

The main chemical composition and physical properties of GGBS are as follows in **Tables 1** and **2**.

Table 1: Chemical composition of GGBS

Chemical composition	CaO	SiO_2	Al_2O_3	Fe_2O_3	MgO	SO_3	K_2O	Na_2O
Content (%)	41.34	32.91	14.61	0.86	5.36	0.4	0.32	0.36

Table 2: Physical properties of GGBS

Density (g/cm^3)	Specific surface area (m^2/kg)	Water content (%)	SO_3 content (%)	28d activity index (%)	Ignition loss (%)
2.9	414	1.3	0.4	105	0.56

Table 3: Chemical composition of tailings from a copper mine

Composition	Fe	Fe^{2+}	FeO	SiO_2	Al_2O_3	CaO	MgO	Cu	S	Loss on ignition
Content (%)	12.43	5.23	6.37	42.97	10.98	6.87	4.69	0.022	0.055	10.383

Table 4: Physical properties of crushed stone

Particle size (mm)	–8 mm		–10 mm		–12 mm	
	Frequency distribution (%)	Negative cumulative distribution (%)	Frequency distribution (%)	Negative cumulative distribution (%)	Frequency distribution (%)	Negative cumulative distribution (%)
–0.15	17.0	17.0	12.8	12.8	8.1	8.1
–0.3 ≈ +0.15	4.6	21.6	5.6	18.4	4.0	12.1
–0.6 ≈ +0.3	10.2	31.8	14.1	32.5	9.2	21.3
–1.18 ≈ +0.6	12.7	44.5	13.8	46.3	13.8	35.1
–2.36 ≈ +1.18	11.6	56.1	10.7	57.0	9.0	44.1
–4.75 ≈ +2.36	24.1	80.2	20.2	77.2	18.6	62.7
–9.5 ≈ +4.75	19.1	99.3	21.2	98.4	34.2	96.9
–16.0 ≈ +9.50	0.5	99.8	1.3	99.7	3.1	100.0
–19.0 ≈ +16						
Packing density	Φ = 0.611		Φ = 0.623		Φ = 0.675	
Porosity (%)	38.9		37.7		32.5	

(2) Graded tailings

The chemical composition of the graded tailings from a copper mine is shown in **Table 3**.

(3) Crushed stone

The physical properties of the crushed stone are provided in **Table 4**.

2.2. Methods

2.2.1. Experimental program

Considering the influencing factors such as the ratio and quality concentration of waste rock tailings, the amount of gel agent added, and the ratio of GGBS to cement, the experiments were conducted on the compressive strength, tensile strength, permeability, and hydration heat of the backfill. The detailed test plan is shown in **Table 5**.

Table 5: Experimental scheme

Aggregate	Mass concentration (%)	Amount of gel agent added (kg/m^3)	Ratio of GGBS to cement
Waste rock tailings ratio = 6:4	80	150, 180, 210, 240, 270, 300	3:7, 4:6, 5:5

2.2.2. Experimental methods

(1) Compressive strength

The compressive strength of the filling body refers to the maximum pressure it can withstand in an unconfined state, which numerically equals the stress required to press the specimen to rupture. The specimens for the compressive strength test of the filling body are prepared indoors. First, considering the mix ratio and concentration requirements for each group of test specimens, a well-mixed slurry is poured into a standard (10 × 10 × 10) cm triple test mold. To ensure that the slurry does not settle during the casting of the test blocks, a method of simultaneous stirring and mold pouring is used. To eliminate bubbles in the specimens, the process involves simultaneous pouring and tamping. The filling body specimens are cured under standard conditions (temperature of 20 °C ± 3°C, relative humidity of 60–80 % for (7, 28 and 60) d before conducting the compressive strength test.

(2) Tensile strength

The tensile strength of the fill material is the ultimate ability of the fill specimens to resist failure under uniaxial tensile stress, which is numerically equal to the maximum tensile stress at failure of a specimen. The preparation method for the specimens used in the uniaxial tensile strength test of the filling body is consistent with that used for preparing the specimens for the compressive strength test of the filling body.

(3) Coulometry (ASTMC1202)

Cylindrical specimens with a height of 50 mm and a diameter of 100 mm are used, and the side of a cylindrical specimen is sealed with wax to achieve the sealing effect. After the test blocks are moist-cured for (7, 28 and 60) d, they are naturally dried and tested for migration electricity. The electricity method test uses a 60 V DC current, with a 0.3 mol/L sodium hydroxide solution as the anode and a 3 % sodium chloride solution as the cathode. The electricity time is 6 h. The current value is measured at regular intervals during the test, and the amount of electricity passing through a sample in 6 h is calculated to determine the chloride ion permeability of the concrete.[25]

(4) Test of hydration heat release characteristics

Testing the hydration heat release characteristics of the GGBS paste fill material requires a TAM Air Isothermal Calorimeter (TA Instruments, USA). It is an 8-channel calorimeter for measuring a sensitive and stable heat flow, with a temperature measurement range of 5–90 °C.

3 RESULTS AND DISCUSSION

3.1 Influence of GGBS on the strength of concrete

The effect of different amounts of gel agent on the strength of the filling body is shown in **Figure 1**.

As shown in **Figure 1**, under standard curing conditions, when the curing time of backfill specimens is 7 d, the strength of the specimens increases with a higher binder content. Within the same group, specimens with 30 % GGBS content demonstrate the highest strength, while those with 50 % GGBS exhibit the lowest strength. This phenomenon is most pronounced in the group with a binder dosage of 180 kg/m^3. At curing times of 28 d and 60 d, the strength of backfill specimens continues to increase with a higher binder content. However, within the same group, specimens with 30 % GGBS now show the lowest strength, whereas those with 50 % GGBS achieve the maximum strength. This indicates that ordinary Portland cement significantly enhances the early-stage strength of backfill materials, while GGBS plays a more substantial role in improving the mid-to-late stage strength.

3.2 Influence of GGBS on concrete durability (tensile strength)

The effect of different amounts of gel agent on the tensile strength of the filling body is shown in **Figure 2**.

During the hardening of concrete, the hydration reaction of cement generates a large amount of heat. However, the rates at which heat dissipates from the interior or the surface of the concrete are different, resulting in a large temperature difference. This can cause uneven temperature deformation and tensile stresses in the concrete. Once the tensile stress exceeds the instantaneous tensile strength of the concrete, cracks occur in the interior or on the surface of the concrete, which is one of the main factors causing early cracking of concrete. These are

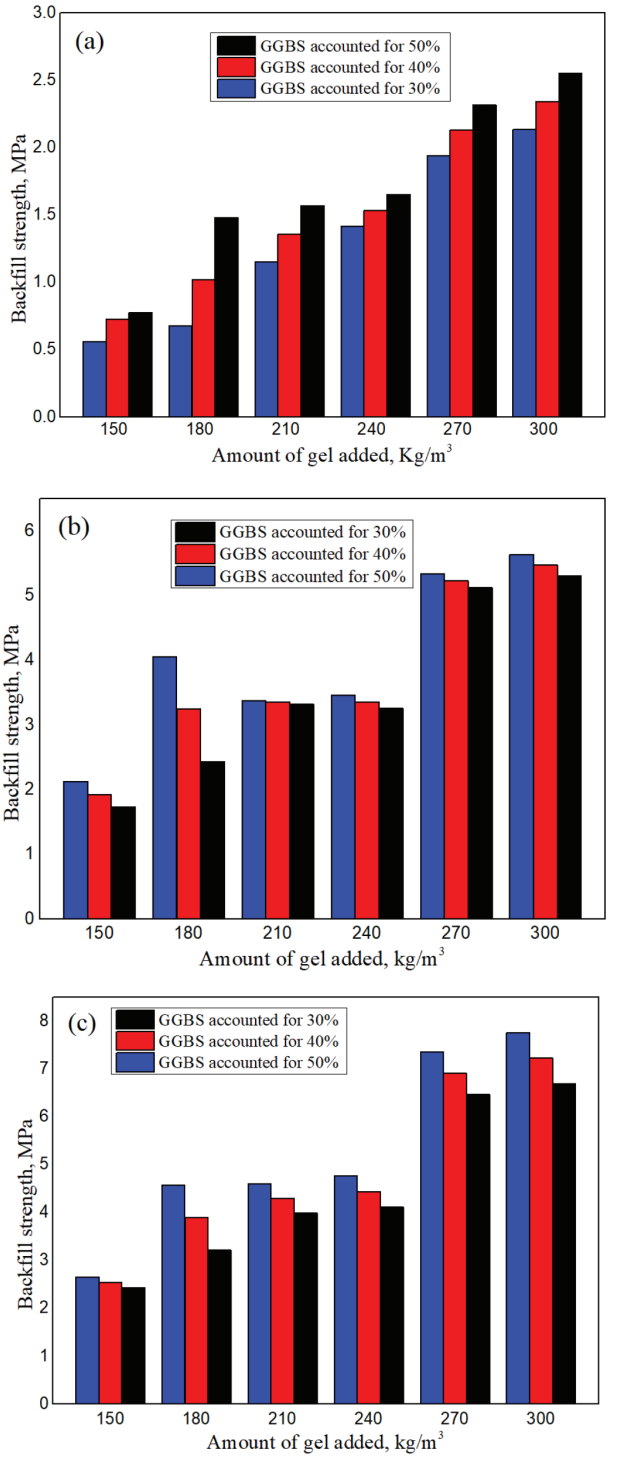

Figure 1: Compressive strength of the backfill after: a) 7 d, b) 28 d, c) 60 d

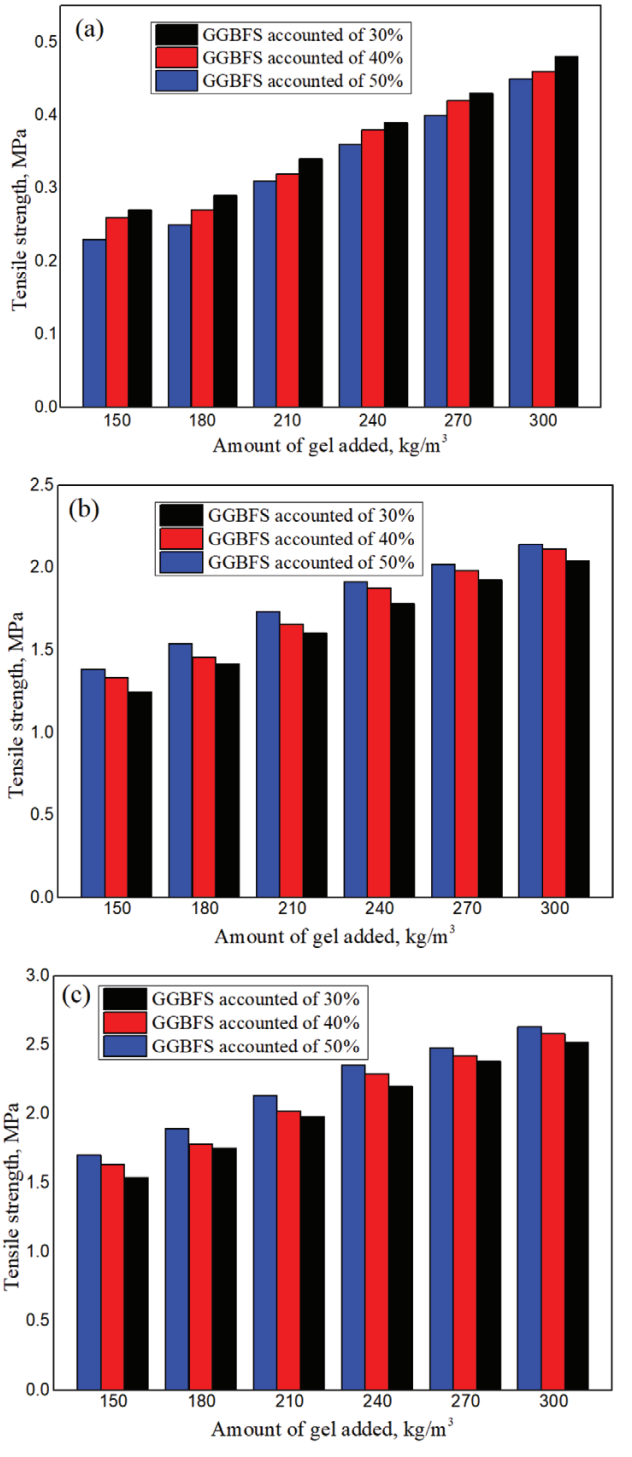

Figure 2: Tensile strength of the backfill after: a) 7 d, b) 28 d, c) 60 d

usually harmful cracks that penetrate concrete, and are very detrimental to the durability of concrete.

As shown in **Figure 2**, when the curing time of the backfill specimens is 7 days, the tensile strength increases with a higher binder content. Within the same group, specimens with 30 % GGBS exhibit the maximum tensile strength, while those with 50 % GGBS show the minimum tensile strength. At curing times of 28 d and 60 d, the tensile strength of the backfill specimens still increases with the higher binder content. However, within the same group, specimens with 30 % GGBS now display the lowest tensile strength, whereas those with 50 % GGBS achieve the highest tensile strength. This indicates that ordinary Portland cement

significantly enhances the early-stage tensile strength of the backfill material, while GGBS plays a more substantial role in improving the mid-to-late stage tensile strength.

3.3 Impermeability of the backfill

When the ratio of waste rock to tailings is 6:4, the mass concentration is 80 %, and the amount of gel agent added is 270 kg/m^3, the compressive and tensile strengths of the filling body after (7, 28 and 60) d all reach high levels. Therefore, the migration charge situation of the filling slurry needs to be observed under these conditions and when the ratios of GGBS in cement are (30, 40 and 50) %, respectively. The change in migration energy of slag filling body in different proportions is shown in **Table 6**.

Table 6: Effect of GGBS on migration energy

Percentage of slag content (%)	Transfer charge (Coulombs, C)		
	7 d	28 d	60 d
30	5123	2894	1532
40	4509	2859	1488
50	3102	2234	1231

The chemical components of GGBS are SiO_2, Al_2O_3, and others. When it is added as an admixture into cement concrete, active SiO_2 and Al_2O_3 can react with the $Ca(OH)_2$ produced by the hydration of C_2S in cement, further forming hydrated calcium silicate products. These products can fill the pores in the cement concrete, greatly increasing its compactness, improving the pore structure, reducing the porosity, and reducing the maximum pore size, resulting in a compact and finely layered self-compacting system. This improves the impermeability of the concrete, and its water permeability is significantly reduced. At the same time, this can also prevent water seepage and segregation.

In this experiment, the migration charge of the concrete specimens decreased gradually with the increase in the GGBS dosage, indicating that adding GGBS can improve the resistance of concrete to chloride ion penetration. Because GGBS participates in the secondary hydration reaction, it generates a relatively stable hydrated calcium silicate gel. The improvement of hydrated products and the filling effect of mineral admixtures make the internal structure of the concrete more compact, reducing the porosity and pore size and blocking the permeation path. For the same curing age, the migration charge of the concrete test block decreases with the increase in the GGBS content, while for the same GGBS content, the migration charge of the test block decreases with the increase in the curing age.

3.4 Hydration heat

Under the conditions where the ratio of waste rock to tailings is 6:4, the mass concentration is 80 %, and the gel additive amount is 270 kg/m^3, four hydration heat test schemes for filling slurry are conducted. These schemes include: a sample with 0 % GGBS (sample A), a sample with 30 % GGBS (sample B), a sample with 40 % GGBS (sample C), and a sample with 50 % GGBS (sample D). This is shown in **Table 7**.

Table 7: Test scheme of hydration heat

Sample	Ratio of waste rock to tailings	Mass concentration, %	Gel additive amount, kg/m^3	Proportion of GGBS, %
A	6:4	80%	270	0
B				30
C				40
D				50

During the hardening of concrete, the hydration reaction of cement produces a large amount of heat, but the dissipation rates of heat from the interior and surface of the concrete are not the same, resulting in a large temperature difference that can cause uneven temperature deformation and generate tensile stress. Once the tensile stress exceeds the instantaneous tensile strength of the concrete, cracks occur inside or on the surface of the concrete, which is one of the main factors of early cracking

Table 8: Hydration heat release stage division

Hydration heat release stage division		Sample			
		A	B	C	D
Rapid reaction stage	Duration, t/h	0.22	0.56	0.59	0.56
	Heat release, Q/J·g^{-1}	3.59	2.27	3.42	1.53
	Rate of heat release, R/J·(g·h)$^{-1}$	13.31	3.82	5.53	2.58
Induction stage	Duration, t/h	2.21	3.58	3.81	6.42
	Heat release, Q/J·g^{-1}	12.01	9.52	12.54	12.89
	Rate of heat release, R/J· (g·h)$^{-1}$	5.32	2.61	3.15	2.01
Acceleration stage	Duration, t/h	8.54	14.72	15.28	10.21
	Heat release, Q/J·g^{-1}	37.6	14.35	15.03	6.32
	Rate of heat release, R/J·(g·h)$^{-1}$	4.41	0.95	0.96	0.61
Deceleration stage	Duration, t/h	108.79	100.85	100.25	102.65
	Heat release, Q/J·g^{-1}	182.23	48.52	48.05	22.82
	Rate of heat release, R/J· (g·h)$^{-1}$	1.65	0.46	0.47	0.22

of concrete. These cracks are usually harmful and can significantly reduce the durability of concrete.

The hydration heat release of the filling material can be divided into five stages: rapid reaction stage, induction stage, acceleration stage, deceleration stage, and stable stage. After organizing the test data, the duration of each stage, as well as the heat release amount and heat release rate values for the four types of samples are shown in **Table 8**.

As shown in the above table, the addition of GGBS to concrete can reduce the hydration heat of the paste. When the addition amount is less than 30 %, the reduction in hydration heat is not significant. However, when the amount reaches 50 %, the hydration heat after 3 d and 7 d is significantly reduced. The hydration dynamics of the GGBS filling material were studied by using the Krstulović-Dabić hydration kinetic model. Some scholars had already carried out relevant research.[26,27] This model is based on the characteristics of the change in the degree of hydration of heterogeneous material systems relative to reaction time.[28,29] It describes the hydration kinetics characteristics by constructing parameters such as degree of hydration and reaction rate. The model assumes three basic hydration processes: nucleation and crystal growth (*NG*), interfacial reactions (*I*), and diffusion (*D*). The kinetic differential equations for these three processes can be written as:

(1) Crystallization nucleation and crystal growth processes (*NG*)

$$\left[-\ln(1-\alpha)\right]^{\frac{1}{n}} = K_{\mathrm{NG}} \cdot (t-t_0) \tag{1}$$

$$\ln\left[-\ln(1-\alpha)\right] = n \cdot \ln K_{\mathrm{NG}} + n \cdot \ln(t-t_0) \tag{2}$$

$$F_{\mathrm{NG}}(\alpha) = n \cdot K_{\mathrm{NG}} \cdot (1-\alpha)\left[-\ln(1-\alpha)\right]^{\frac{n-1}{n}} \tag{3}$$

(2) Phase boundary action process (*I*)

$$1-(1-\alpha)^{\frac{1}{3}} = K_1 \cdot (t-t_0) \tag{4}$$

$$\ln\left[1-(1-\alpha)^{\frac{1}{3}}\right] = \ln K_1 + \ln(t-t_0) \tag{5}$$

$$F_1(\alpha) = 3 \cdot K_1 \cdot (1-\alpha)^{\frac{2}{3}} \tag{6}$$

(3) Diffusion process (*D*)

$$\left[1-(1-\alpha)^{\frac{1}{3}}\right]^2 = K_{\mathrm{D}} \cdot (t-t_0) \tag{7}$$

$$2\ln\left[1-(1-\alpha)^{\frac{1}{3}}\right] = \ln K_{\mathrm{D}} + \ln(t-t_0) \tag{8}$$

$$F_{\mathrm{D}}(\alpha) = \frac{3 \cdot K_{\mathrm{D}} \cdot (1-\alpha)^{\frac{2}{3}}}{\left[2-2 \cdot (1-\alpha)^{\frac{2}{3}}\right]} \tag{9}$$

In the equations, α represents the degree of hydration reaction, while K_{NG}, K_{I}, and K_{D} are the reaction rate constants for the *NG*, *I*, and *D* processes, respectively. $F_{\mathrm{NG}}(\alpha)$, $F_{\mathrm{I}}(\alpha)$, and $F_{\mathrm{D}}(\alpha)$ are the hydration reaction rates for the *NG*, *I*, and *D* processes, respectively, while $t–t_0$ is the time from the start of the acceleration phase for hydration, and n is the reaction index that describes geometric crystal growth.

The hydration reaction of the filling material can be characterized with the hydration reaction degree α and the hydration reaction rate $\mathrm{d}\alpha/\mathrm{d}t$, which can be determined using Equations (10) and (11), by converting the heat release rate and heat release data obtained with isothermal calorimetry testing into the required parameters of the dynamic model.

$$\alpha_{(t)} = \frac{Q_{(t)}}{Q_{\max}} \tag{10}$$

$$\frac{\mathrm{d}\alpha}{\mathrm{d}t} = \frac{\mathrm{d}Q/\mathrm{d}t}{Q_{\max}} \tag{11}$$

In the equations, $Q_{(t)}$ represents the amount of heat released from the beginning of the acceleration period to time t, while $Q_{\max}$ represents the maximum heat released when the hydration of the filling material is terminated. It can be obtained using TAM IV Lab Asst software attached to the TAM Air isothermal microcalorimeter to read the maximum heat released when the sample's hydration is terminated. The $Q_{\max}$ for sample A is 210.41, while for samples B–D, it is 82.83, 75.14, and 41.52, respectively. By substituting $Q_{\max}$ into Equations (10) and (11), the degree of hydration and hydration rate at time t can be calculated. Then, by substituting α into Equations (2), (5), and (8), the kinetic parameters n, K_{NG}, K_1, and K_{D} for samples A–D can be obtained through linear fitting, as shown in **Table 9**.

Table 9: Hydration kinetics parameters of samples A–D at (20±2) °C

Sample	n	K_{NG}	K_1	K_{D}
A	1.6156	0.03795	0.00878	0.00206
B	1.2589	0.02468	0.00659	0.00258
C	1.2478	0.02425	0.00623	0.00252
D	1.165	0.01856	0.00447	0.00322

From **Table 9**, it can be observed that as the cement content decreases, the value of n decreases, and the value of K_{NG} also decreases. From the chemical reaction perspective, the *NG* process belongs to autocatalytic reaction, and its chemical reaction rate is not only affected by the number of reactants, but also by the amount of reaction product generated. After adding GGBS, on the one hand, the reduction in cement leads to a decrease in the amount of Ca^{2+} released and a decrease in the effective sulfate content in the solution; on the other hand, Ca^{2+} is adsorbed on the surface of GGBS particles, which delays the formation of hydration products such as $Ca(OH)_2$ and AFt nuclei. The value of K_I decreases with the decrease

in cement and the increase in the GGBS dosage. When C_3S particles come into contact with water, a calcium-deficient silicon-rich layer is formed on their surfaces, and then Ca^{2+} is adsorbed around them to form a double electric layer, hindering the dissolution of C_3S particles. However, when $Ca(OH)_2$ in the solution becomes supersaturated, the potential decreases, the double electric layer disappears, and C_3S dissolution is promoted.

When GGBS appears in the liquid phase, Ca^{2+} is more likely to be adsorbed on the surface due to a larger specific surface area, which prolongs the time required for $Ca(OH)_2$ in the liquid phase to reach supersaturation and weakens the effect of interfacial interaction. The value of K_D increases with the decrease in the cement content and the increase in GGBS. The reason for this is that with the prolongation of the hydration time, hydration products continue to form and grow, gradually forming a microstructure layer of hydration products on the surface of particles. In the middle and late stages of hydration, the microstructure layer gradually becomes denser, resulting in a decrease in the space for further growth of hydration products and also a decrease in the hydration reaction rate; thus, the hydration reaction gradually becomes controlled by diffusion. Due to the early hydration inertness of GGBS, the hydration products generated in the system are significantly fewer than those of pure cement. This indicates that the structural space is larger and the anti-diffusion ability is lower, so the K_D value increases.

4 CONCLUSIONS

This study included experiments based on different combinations of GGBS and cement as the binders. The effects of the GGBS content on the compressive strength, tensile strength, impermeability, and hydration reaction of the backfill material were investigated. The main findings and conclusions are summarized below:

(1) As the binder content increases, the compressive and tensile strengths of the backfill material improve. A higher proportion of ordinary Portland cement significantly enhances the early-stage compressive and tensile strengths, while a higher GGBS content markedly improves the mid-to-late stage compressive and tensile strengths. Notably, when the binder dosage is (180, 210 or 240) kg/m³, the compressive strength of the backfill shows no significant difference. However, when the binder dosage reaches 270 kg/m^3, the compressive strength increases substantially. The tensile strength of the backfill follows a linear improvement pattern with increasing binder content.

(2) A higher GGBS content reduces the migration charge of the backfill material, thereby strengthening its chloride ion penetration resistance. The concrete hardened with GGBS has good resistance to sulfate, chloride ion, and alkali attacks, and can significantly improve long-term strength and durability.

(3) The strength of the fill material during coagulation and hardening of the GGBS paste is related to the decrease in the porosity and increase in the strength of the fill material. As the hydration time increases, the porosity decreases and the strength increases. With the joint influence of the reduction in the cement content and the early hydration inertness of GGBS, the hydration reaction rate inside the fill material decreases significantly, resulting in a lower early strength due to the reduced amount of hydration products. As the GGBS's activating effect gradually takes effect, the interfacial forces and diffusion processes at adjacent boundaries become active, accelerating the hydration reaction and enhancing the later strength of the fill material.

Acknowledgment

This research was supported by the Tianjin University of Technology research start-up funds.

6 REFERENCES

[1] G. Chen, N. Yao, Y. C. Ye, F. H. Fu, N. Y. Hu, Z. Zhang, Influence of partial cement substitution by ground blast furnace slag on the mechanical properties of phosphogypsum cemented backfill, Environ. Sci. Pollut. R., 30 (**2023**), 102972–102985, doi:10.1007/s11356-023-29629-9

[2] Q. S. Chen, L. Z. Gao, A. X. Wu, Y. Feng, Y. B. Tao, D. L. Wang, Alkaline-washed phosphogypsum-based cemented paste backfill prepared using steel slag and blast furnace slag: Mechanical properties, fluoride immobilization, and hydration mechanism, Case Stud. Constr. Mater., 21 (**2024**), e04028, doi:10.1016/j.cscm.2024.e04028

[3] T. A. Fatah, R. J. Zhang, Y. Miao, A. K. Mastoi, X. S. Huang, N. N. Wurie, Strength and leaching behavior of tailing-based paste backfill at high water content amended with lime activated ground granulated blast furnace slag and flocculant, Environ. Sci. Pollut. R., 31 (**2024**), 11115–11127, doi:10.1007/s11356-024-31866-5

[4] X. Y. He, W. L. Li, J. Yang, Y. Su, Y. N. Zhang, J. Y. Zeng, H. B. Tan, Multi-solid waste collaborative production of clinker-free cemented iron tailings backfill material with ultra-low binder-tailing ratio, Constr. Build. Mater., 367 (**2023**), 130271, doi:10.1016/j.conbuildmat.2022.130271

[5] M. Zhu, G. Xie, L. Liu, R. Wang, S. Ruan, P. Yang, Z. Fang, Strengthening mechanism of granulated blast-furnace slag on the uniaxial compressive strength of modified magnesium slag-based cemented backfilling material, Process Saf. Environ., 174 (**2023**), 722–733, doi:10.1016/j.psep.2023.04.031

[6] X. B. Ji, X. Z. Gu, Z. R. Wang, S. Xu, H. Q. Jiang, E. Yilmaz, Admixture effects on the rheological/mechanical behavior and micro-structure evolution of alkali-activated slag backfills, Minerals, 13 (**2023**), 30, doi:10.3390/min13010030

[7] B. T. Li, Z. R. Liu, Q. Sun, L. Yang, Preparation of alkali-activated nickel slag-based cemented tailings backfill: Workability, strength characteristics, localized deformation and hydration mechanism, Constr. Build. Mater., 411 (**2024**), 134639, doi:10.1016/j.conbuildmat.2023.134639

[8] K. Li, L. S. Zhu, Z. H. Wu, X. M. Wang, Properties of Cemented Filling Materials Prepared from Phosphogypsum-Steel Slag-Blast-Furnace Slag and Its Environmental Effect, Materials, 17 (**2024**), 3618, doi:10.3390/ma17143618

[9] Q. Chen, S. Sun, Y. Wang, Q. Zhang, L. Zhu, Y. Liu, In-situ remediation of phosphogypsum in a cement-free pathway: Utilization of ground granulated blast furnace slag and NaOH pretreatment,

Chemosphere, 313 (**2023**), 137412, doi:10.1016/j.chemosphere.2022.137412

[10] A. M. A. Mohammed, O. Husain, M. Abdulkareem, N. Z. Mohd Yunus, N. Jamaludin, E. Mutaz, M. Hamdan, Explainable Artificial Intelligence for predicting the compressive strength of soil and ground granulated blast furnace slag mixtures, Results Eng., 25 (**2025**), 103637, doi:10.1016/j.rineng.2024.103637

[11] C. H. Liu, Z. Y. Li, A. Bezuijen, L. H. Chen, P. Cachim, Optimizing the shield tunnel backfilling grouts with supplementary gel agents by response surface methodology, Constr. Build. Mater., 421 (**2024**), 135575, doi:10.1016/j.conbuildmat.2024.135575

[12] S. L. Liu, Y. M. Wang, A. X. Wu, D. Q. Shi, S. X. Yang, Z. Ruan, M. Z. Zhang, Early mechanical strength, hydration mechanism and leaching behavior of alkali-activated slag/GGBS paste filling materials, J. Build. Eng., 84 (**2024**), 108481, doi:10.1016/j.jobe.2024.108481

[13] R. F. Ma, G. J. Wang, Q. Sun, Preparation and strength formation mechanism of alkali-stimulated spontaneous combustion gangue-granulated blast furnace slag backfill, Environ. Sci. Pollut. R., 31 (**2024**), 772–784, doi:10.1007/s11356-023-30893-y

[14] X. Wang, J. Lv, J. Yang, J. Zhu, B. He, X. Wang, X. Bai, Synergistic effects of ground granulated blast furnace slag and circulating fluidized bed GGBS in lime-activated gel agents, Case Stud. Constr. Mater., 22 (**2025**), e04259, doi:10.1016/j.cscm.2025.e04259

[15] A. D. Pan, M. Grabinsky, Effect of submerged curing on properties of cemented paste backfill, Int. J. Min. Reclam. Environ., 37 (**2023**), 1016–1028, doi:10.1080/17480930.2023.2273030

[16] H. T. Pang, W. Y. Qi, Q. X. Zhao, Y. L. Huang, D. Z. Zhao, H. Q. Song, Y. Yu, A novel alkali-slag cemented tailings backfill: Recycling of soda residue and calcium carbide slag, Constr. Build. Mater., 445 (**2024**), 137875, doi:10.1016/j.conbuildmat.2024.137875

[17] Q. S. Ren, W. Y. Qi, Q. X. Zhao, Y. L. Jia, Y. B. Feng, Y. J. Han, H. T. Pang, Preparation and characterization of low-carbon gel agents based on soda-residue-activated ground granulated blast-furnace slag: A case study on cemented paste backfills, Metals, 13 (**2023**), 694, doi:10.3390/met13040694

[18] C. J. Wang, P. Y. Chen, C. Wang, Investigation on the basic performance of the sustainable alkali-activated slag blended with sulphidic copper tailings, Case Stud. Constr. Mater., 20 (**2024**), e02844, doi:10.1016/j.cscm.2023.02844

[19] R. G. Gao, K. P. Zhou, J. L. Li, Research of the mechanisms of backfill formation and damage, Mater. Tehnol., 52 (**2018**), 163–169, doi:10.17222/mit.2017.070

[20] D. L. Wang, Y. B. Tao, Y. Feng, D. B. Zhu, Q. L. Zhang, Q. S. Chen, Enhanced solidification/stabilization (S/S) of fluoride in smelting solid waste-based phosphogypsum cemented paste backfill utilizing biochar: Mechanisms and performance assessment, J. Environ. Manage., 367 (**2024**), 122088, doi:10.1016/j.jenvman.2024.122088

[21] S. J. Wang, Y. Sun, Z. B. Li, K. Xiao, W. Cui, Experimental study on modified low liquid limit silt for abutment backfill in bridge-embankment transition section, Geomech. Eng., 32 (**2023**), 601–613, doi:10.12989/gae.2023.32.6.601

[22] S. Q. Yu, H. Q. Jiang, Z. Y. Xi, X. P. Li, P. Wang, Y. Fu, Image analysis as a geometry- and integrity-independent tool for predicting strength of cemented tailings backfill using slag-based binder, Constr. Build. Mater., 444 (**2024**), 137867, doi:10.1016/j.conbuildmat.2024.137867

[23] T. Mashifana, T. Sithole, Clean production of sustainable backfill material from waste gold tailings and slag, J. Clean. Prod., 308 (**2021**), 127357, doi:10.1016/j.jclepro.2021.127357

[24] N. Ouffa, T. Belem, R. Trauchessec, P. Lemoine, Y. Benarchid, M. Benzaazoua, Water quenching and grinding of ladle furnace slag for use as supplementary cementitious material in cemented mine backfills, Cement Concrete Comp., 160 (**2025**), 106048, doi:10.1016/j.cemconcomp.2025.106048

[25] T. Gehlot, S. S. Sankhla, S. Parihar, Compressive, flexural strength test and chloride ion permeability test of concrete incorporating quartzite rock dust, Mater. Today Proc., 45 (**2021**), 4724–4730, doi:10.1016/j.matpr.2021.01.166

[26] G. J. Zhu, W. C. Zhu, C. Hou, H. Q. Jiang, Use of Saline Water in Cemented Fine Tailings Backfill with One-Part Alkali-Activated Slag, J. Mater. Civ. Eng., 35 (**2023**), 04022472, doi:10.1061/(ASCE)MT.1943-5533.0004612

[27] R. Krstulović, P. Dabić, A conceptual model of the cement hydration process, Cem. Concr. Res., 30 (**2000**), 693–698, doi:10.1016/S0008-8846(00)00231-3

[28] V. B. R. Suda, P. Srinivasa Rao, Experimental investigation on optimum usage of Micro silica and GGBS for the strength characteristics of concrete, Mater. Today Proc., 27 (**2020**), 805–811, doi:10.1016/j.matpr.2019.12.354

[29] C. Min, Y. Shi, Z. Liu, Properties of cemented phosphogypsum (PG) backfill in case of partial substitution of composite Portland cement by ground granulated blast furnace slag, Constr. Build. Mater., 305 (**2021**), 124786, doi:10.1016/j.conbuildmat.2021.124786